

N 70 18743

NASA CR 108094

Division of Engineering
Brown University
Providence, Rhode Island

CASE FILE COPY

MIDWAY REPORT

Investigation of the Effects of
Sub-Threshold High Energy Electrons on
the Properties of Silicon Photovoltaic Cells

Contract 952386

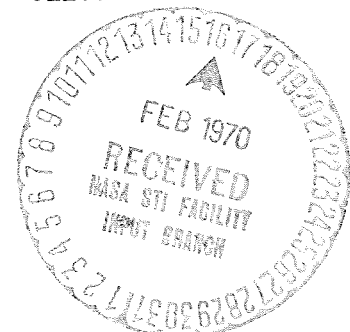
Period Covered:

February 3, 1969 through August 3, 1969

Report prepared by: J. J. Loferski and E. E. Crisman

Sponsored by: Jet Propulsion Laboratory
California Institute of Technology
4800 Oak Grove Drive
Pasadena, California 91103

September 1969



Division of Engineering
Brown University
Providence, Rhode Island

MIDWAY REPORT

Investigation of the Effects of
Sub-Threshold High Energy Electrons on
the Properties of Silicon Photovoltaic Cells

Period Covered:

February 3, 1969 through August 3, 1969

Report prepared by: J. J. Loferski and E. E. Crisman

Sponsored by: Jet Propulsion Laboratory
California Institute of Technology
4800 Oak Grove Drive
Pasadena, California 91103

September 1969

ABSTRACT

The effects of irradiating semiconductors by "sub-threshold" electrons is reviewed. It is pointed out that lithium atoms dissolved in silicon would be displaced by electrons whose energy is less than 35 keV, whereas the electron must have about 150 keV to displace a silicon atom. Experiments designed to test this phenomenon are described. The effects of electron irradiation on semiconductor surfaces are also reviewed. Experimental apparatus for investigation of the effects of electrons irradiation in organic vapor free vacua (like those of outer space) on the characteristics of silicon photovoltaic cells is described.

<u>TABLE OF CONTENTS</u>	<u>Page No.</u>
INTRODUCTION	1
POSSIBLE BULK EFFECTS OF "SUB-THRESHOLD" ELECTRON IRRADIATION	1
SURFACE EFFECTS OF ELECTRON IRRADIATION	3
REVIEW OF EARLIER EXPERIMENTS ON THE EFFECTS OF SUB-THRESHOLD ELECTRONS ON Ge AND Si	7
EXPERIMENT ARRANGEMENT	9
CONCLUSIONS	11
REFERENCES	12

FIGURE TITLES

- FIGURE 1. Energy level diagram for n-Si surface before and after alteration of the ambient.
- FIGURE 2. Plot of s/s_{\max} vs. surface potential ϕ_s for the case where the capture cross sections for holes and electrons are equal.
- FIGURE 3. Energy band diagram for p-Si surface with inversion layer before and after alteration of the ambient.
- FIGURE 4. I_{sc}/I_{sc0} vs. integrated flux of 115-keV electrons for 1 Ω cm, nSi. Three successive runs. [After Kasai¹⁰]
- FIGURE 5. I_{sc}/I_{sc0} vs. integrated flux of 115 keV electrons for 1 Ω cm, p-Si [After Kasai¹⁰]
- FIGURE 6. Stainless steel irradiation chamber, assembly drawing.
- FIGURE 7. Stainless steel irradiation chamber, photograph.
- FIGURE 8. Photograph of apparatus for low temperature irradiation of silicon p/n cells.

INTRODUCTION

The purpose of the research program supported by this contract is to study the effects of "sub-threshold energy" electrons on the properties of silicon photovoltaic cells, especially silicon cells doped with lithium. By "sub-threshold energy" electrons, we mean electrons whose energies are below the minimum energy E_{th} required to produce observable changes in the electronic properties of photovoltaic cells by displacement of the host lattice (Si) atoms.

The changes by electrons whose energies exceed the threshold energy E_{th} are deleterious; they result in a degradation of the power output capability of photovoltaic cells. These changes in electronic properties arise as a result of the introduction of new defects into the semiconductor. The levels produced in silicon by irradiation with electrons above the "damage threshold" are distributed throughout the forbidden energy gap, i.e. both shallow and deep levels appear after irradiation. Shallow levels can change the conductivity σ of the semiconductor and deep levels can affect both σ and the lifetime of minority carriers τ . In "as-grown", high quality silicon like that used in solar cells, τ is controlled by deep-level defect concentrations $\leq 10^{12}/cc$, whereas σ is controlled by shallow level concentrations $\geq 10^{15}/cc$. Therefore, a given deep-level which can affect σ by trapping majority carriers or τ by offering recombination sites for minority carriers is more likely to cause observable changes in τ before it produces any effect on σ . Because τ and σ can be controlled by different kinds of defects, it is possible that the damage thresholds may be different for these two parameters. In the case of silicon, however, the damage thresholds are the same for σ and τ , but a different threshold has been found for n- and p-type materials. [See paper by Flicker, Scott-Monck and Loferski,⁽¹⁾ and doctoral dissertation of R. L. Novak, University of Pennsylvania.⁽²⁾] The earlier investigations showed that the damage threshold in n-Si is 115 keV and that its value in p-Si was 225 keV.

This difference exists because the deep-level defects which control τ and σ in irradiated n-silicon consist of complexes formed by a single vacancy and an impurity atom like O, P, As, etc., while the deep-level defects which control τ and σ in irradiated p-Si are divacancies formed not by the combination of two separately produced vacancies, but rather by the displacement of two adjacent silicon atoms as a result of a scattering event in which sufficient energy is transferred to a silicon atom so that it can displace both itself and one of its neighbors. Obviously, it takes more energy to displace a pair of atoms than to displace a single one. This accounts for the difference in damage thresholds in n- and p-Si.

POSSIBLE BULK EFFECTS OF "SUB-THRESHOLD" ELECTRON IRRADIATION

It is possible in principle for the electron irradiation to produce changes in the electronic properties of a semiconductor even if the electron energy is below that required to displace a host lattice atom. For example, if the crystal contains substitutional impurities whose mass

is smaller than that of the host atom, these lighter atoms could be displaced and vacancies would be produced by electrons whose energy was too low to displace a host lattice atom. For example, lithium atoms have atomic weights of 6 and 7, whereas silicon atoms have atomic weights of 28 and 29.

It can be shown⁽³⁾ that the threshold energy of the electron E_{th} is related to the minimum energy T_m constraining an atom to its site by the relation

$$T_m = \frac{2 (E_{th} + 2mc^2) E_{th}}{Mc^2} \quad (1)$$

where m is the electron mass; M is the mass of the displaced atom and c is the velocity of light. Substitution of appropriate constants in Eq. (1) leads to the more convenient form

$$T_m = \frac{2147.8}{A} (E_{th} + 1.0220) E_{th} \quad (2)$$

where A is the atomic weight of the target atom; E_{th} is the energy of the electron in MeV and T_m is the energy transferred to the struck atom in eV. In the case of silicon, as noted above, the value of E_{th} for displacement of a single silicon atom is 115 keV.⁽¹⁾ Since the atomic weight of silicon is ~ 28 , substitution in Eq. (2) leads to a value for $T_m \sim 12.8$ eV. This is the energy with which Si is bound to its site in the diamond lattice.

If the Li atom occupies a substitutional site and it is bound to that site with the same energy as the Si atom (~ 12.8 eV), then Li atoms would be displaced from such substitutional sites by electrons with energy $E \sim 30$ keV. If the Li atom occupies an interstitial site, even less energy should be needed to displace it.

A factor which argues against easy observation of changes in σ or τ associated with the displacement of Li atoms is the small concentration of Li relative to the concentration of host lattice silicon atoms. In Li-doped solar cell quality n-Si, whose free electron concentration n is assumed to arise from the ionization of Li atoms, the Li ion concentration is, in the range 10^{15} to 10^{16} atoms/cc, i.e., one ionized Li atom per 10^6 or 10^7 Si atoms. The techniques used to measure τ and σ would need to be extremely sensitive if effects of Li displacement are to be observed. However, work by other authors⁽⁴⁾ has shown that the Li concentration in Si is higher than the free electron concentration n . In other words, every Li atom does not contribute an electron to the conduction band. Some Li atoms may have formed electronically inactive complexes with oxygen or other trace impurities in the silicon. Other Li atoms may have precipitated at dislocations where they may form clusters consisting of large number of Li atoms. Electron irradiation could dislodge Li from any of these sites so that the number of Li atoms available for displacement by "sub-threshold" electrons is actually substantially higher than number of Li^+ ions, i.e. than the free carrier concentration.

Another open question which can be answered by irradiation of Si:Li with "sub-threshold" electrons is whether dislodging Li from complexes, substitutional sites, dislocations, etc., improves or degrades τ . If Li atoms are liberated from the sites at which they are lodged, they may migrate through the lattice to form lifetime controlling complexes whose properties result in higher values of τ than those observed in the Si before irradiation. To see why this is so, note that τ is given by the relation⁽¹⁾

$$\frac{1}{\tau} = \sum_i N_{ri} \sigma_{ci} v f_i(E_F) \quad (3)$$

here N_{ri} is the concentration of the i -th recombination center; σ_{ci} is its minority carrier capture cross-section and $f_i(E_F)$ is the probability that a center is occupied by a majority carrier. The value of $f_i(E_F)$ depends on the energy difference between the Fermi energy E_F and the recombination center energy E_r and on the absolute temperature T . Equation (3) is based on the assumption that the recombination centers act independently of each other. Usually, one type of recombination center dominates because the product of the parameters in Eq. (3) is much greater for one kind of defect than for any other kind. If Li atoms dislodged by the "sub-threshold energy" electrons form new complexes with the dominant defect, they could shift the control of lifetime to some other defect species with a consequent increase in τ . Recall that τ is controlled by very small recombination center concentrations, i.e., $N_r \sim 10^{10} - 10^{12}/\text{cc}$. The Li atom concentration in silicon, which may be about $10^{18}/\text{cc}$, is high enough to play a significant role in lifetime control.

Radiation defects resulting from the displacement of impurity atoms have never been observed in a semiconductor. It was proposed at one time that "sub-threshold energy" electron damage in Ge resulted from the displacement of hydrogen atoms dissolved in the Ge but subsequent experiments failed to support this hypothesis.⁽⁵⁾ It should, however, be pointed out that there have been virtually no investigations aimed at observing this phenomenon. The large mass difference between Li and Si atoms provides a favorable situation for studying impurity displacement effects. (Of course, the situation would be even more favorable in Ge whose isotopes have atomic weights ranging from 70 to 76.)

A search for effects of Li displacements on the properties of Si is of importance to solar cell utilization. Calculation of the number of displacements may have to take into account Li atom displacements. In addition, a study of Li displacement phenomena could elucidate the mechanism for self-healing of radiation damage in Li doped silicon.

SURFACE EFFECTS OF ELECTRON IRRADIATION

In the preceding section we have discussed possible bulk effects of irradiation of silicon by electrons whose energy is too low to displace silicon atoms. The displacement of Li impurities may or may not lead to

observable changes in σ and τ . However, there is no question about the ability of sub-threshold electrons to cause changes in the surface properties of semiconductors including silicon. These effects may be transient or permanent. They will be strong functions of the gaseous ambient in which the semiconductor is immersed and they are usually strong functions of the past history of the surface.

We shall first present a brief discussion of the role played by the surface in affecting the electronic properties of the semiconductor. The surface is commonly characterized by a surface recombination velocity s or its equivalent, a surface lifetime τ_s . For example, if one measures the decay time of a photoconductive signal in a semiconductor filament, the lifetime is in fact an "effective lifetime" τ_{eff} which is related to the bulk lifetime τ_b and the surface lifetime τ_s by the relation

$$\frac{1}{\tau_{\text{eff}}} = \frac{1}{\tau_b} + \frac{1}{\tau_s} \quad (4)$$

The surface lifetime τ_s is related to s by the following expression

$$\frac{1}{\tau_s} = \frac{s}{2w} \quad (5)$$

where w is the thickness of the filament (its smallest dimension).

The surface recombination velocity is a function of the number of recombination sites residing on the surface; on the energy level (or levels) of these recombination centers and on the energy difference between the Fermi level and the recombination centers. The position of the Fermi level at the surface depends on its position in the bulk material, i.e. on the level of doping, and on the surface potential ϕ_s , i.e. the "bending" of the bands at the surface. Figure 1 illustrates a possible configuration of bands before and after changes in the ambient for the case of n-Si. In this figure, the surface region consists of an inversion layer, i.e. the Fermi level at the surface lies below E_i , the Fermi level in intrinsic material and, therefore, the surface is p-type. The degree of band bending depends on the "slow" states located on the outside of, or inside the thin ($< 1000 \text{ \AA}$) oxide layer which is always present on silicon after exposure to the atmosphere. In order to produce the inversion layer shown in Fig. 1, the "slow" states have to be acceptors. They are neutralized by conduction band electrons which leave the interior of the specimen and travel through the oxide until they reach the acceptor defects and neutralize them.

Surface lifetime and, therefore, the surface recombination velocity is controlled by the "fast" states. In Fig. 1, there is an implicit assumption that the fast states are all at a single energy level E_t ; this is not necessarily so. Just as in the bulk, it is possible that there may be a number of different kinds of recombination centers, each characterized by its own cross section for capture of minority carriers. The surface lifetime will then be determined by an expression analogous to Eq. (3).

There is, however, an important difference between the situation in the bulk and at the surface. The bulk Fermi level is fixed relative to the bands and it can be changed only with difficulty. The principal method for changing the position of the Fermi level in the bulk and, therefore, the occupancy factor $f_i(E_F)$ in Eq. (3) and consequently changing the dominant recombination center, is to change the level of doping.

Changing the occupancy factor $f_i(E_F)$ of the surface recombination sites requires a change in the "doping" of the surface which of course is easily accomplished. Subjecting the surface to different etchants, or exposing the etched surface to different ambients (vacuum, dry O_2 , moist O_2 etc.) can easily change the acceptor state population on the surface and inside the oxide. This in turn can change the surface potential ϕ_s as shown in Fig. 1, where it is assumed that dry air has caused an increase in slow state acceptor levels and, therefore, a change in ϕ_s . This could lead to a change in the occupancy factor $f_i(E_F)$ of Eq. (1). If the change in ϕ_s is large enough, this could result in a different set of recombination centers predominating.

Now irradiation of a semiconductor by sub-threshold electrons can change both the "slow" state population and the fast state population. It can change the slow state population a) by dislodging atoms from the outermost layers of the oxide layer; b) by displacing atoms inside the oxide and thus introducing new defects; and c) by ionizing atoms of the ambient gases which then are adsorbed on the surface of the oxide layer. It can change the fast state population by dislodging atoms in the "surface" layer and thereby producing defects similar to those introduced into the bulk. In the case of silicon, since the surface layer is an oxide of silicon, the defects produced near the surface ought to be mainly A-centers, i.e. oxygen plus vacancy, even in floating-zone silicon which would have very few A-centers in its interior after electron irradiation. Of course, it is not evident that the "surface A-center" would have the same properties as the bulk A-center. The surface region is characterized by dangling silicon bands. Even after the oxygen atoms have been incorporated, there will still be a transition region between the Si and the oxide comprising most of the surface film, so that "surface A-center" properties could be special.

The experimental problem is therefore to separate radiation-produced changes in surface potential ϕ_s from changes in the nature of the recombination centers. Examination of the theory of surface recombination velocity as a function of ϕ_s , E_t , E_F suggests ways of separating these effects. According to this theory, the ratio of s to its maximum value s_{max} is given by

$$\frac{s}{s_{max}} = \frac{\cosh[(E_t - E_i)/kT - u_o] + 1}{\cosh[(E_t - E_i)/kT - u_o] + \cosh(u_s - u_o)} \quad (6)$$

In this expression, $u_o = \frac{1}{2} \ln(\sigma_p/\sigma_n)$ and u_s is the dimensionless surface potential $u_s = e \phi_s / kT$.

Figure 2 shows a plot of Eq. (6), i.e. of s/s_{max} vs. ϕ_s (or u_s) for two different recombination centers and for the case $\sigma_p = \sigma_n$ and,

therefore, $u = 0$. A change in position of the dominant recombination center by 0.1 eV would lead to a 50% increase in the half width of this curve.

Generation of a curve like that shown in Fig. 2 requires that a parameter proportional to the surface recombination velocity be measured and that an independent means of changing the surface potential be available. It is not necessary to measure either ϕ_s or s absolutely; it is only necessary to measure parameters proportional to them.

The parameter proportional to s which we have chosen to measure is the photovoltaic short circuit current I_{sc} produced by strongly absorbed light. As we have previously pointed out, (9)

$$1/I_{sc} = As + B \quad (7)$$

where A and B are constants, provided that the light is very strongly absorbed ($\alpha\ell \gg 1$ where ℓ is the distance between the surface on which the light is incident and the junction, and α is the absorption constant) and that the minority carrier diffusion length L satisfies the relation $\ell/L \leq 1$.

In a series of previously described experiments, we have reported the very substantial changes which occur in I_{sc} for both silicon and germanium surfaces as a result of irradiation. Figures 4 and 5 show typical sets of data for Si photocells. In Fig. 4, I_{sc} increases as a result of irradiation; in Fig. 5 the reverse is true. The 40% increase shown in Fig. 4 would require a decrease of at least 40% in s . The 40% decrease in I_{sc}/I_{sc0} shown in Fig. 5 would require a 40% increase in s . As was stated above, this change in s could occur either with ϕ constant or with ϕ changing. Even with ϕ constant one or both of two mechanisms can be active. First of all, as shown in Fig. 2, a change in the nature of the recombination centers could lead to substantial changes in s . Secondly, even if the radiation were simply producing more recombination levels of the same kind as those originally present, s would increase because s is proportional to the number of recombination centers at the surface. (11)

In view of these considerations, it is very likely that electron bombardment changes the character and concentration of both slow and fast states. The best way to resolve the issue is to generate curves like those shown in Fig. 2 before and after electron irradiation.

There are a number of ways to produce such curves. The basic idea is to change the surface potential by applying a field transverse to the surface. Using this technique, Many and Gerlick¹¹ succeeded in applying a field large enough to generate a curve like that shown in Fig. 2. They computed the surface recombination velocity from measurements of effective lifetime based on pulse injection techniques. In their experiments, they exposed the surface to different ambients and were able to measure both the change in surface potential and the activation energy of the recombination centers caused by different ambients.

Dousmanis¹² obtained an oscilloscope display of curves like those shown in Fig. 2 by means of the following procedure. He placed a thin sheet of mica, one side of which was covered by a semitransparent metal layer on the surface of a diode opposite the plane of the p-n junction. He applied a reverse bias to the junction and measured the reverse saturation current I_0 of this p-n junction. Under certain conditions (which were satisfied for his particular junctions), I_0 is directly proportional to s . The signal proportional to I_0 was displayed on the vertical deflection plates of the oscilloscope. A large a.c. voltage was applied between the metallized side of the mica and the body of the semiconductor. The a.c. signal was proportional to ϕ_s ; it was applied across the horizontal plates of the oscilloscope. In his experiments, the signal on the scope face proved to be only a segment of the curve shown in Fig. 2 because the mica was so thick that only a small fraction of the applied a.c. potential appeared across the very thin ($\sim 1000 \text{ \AA}$) surface oxide region. Consequently only small changes were induced in ϕ_s .

In adapting these techniques to our particular problem, we intend to place a fine wire mesh screen a few mils above the silicon surface. The electric field required to change ϕ_s by one volt is $2 \times 10^6 \text{ V/cm}$. This would require a potential difference of about 500 V between the screen and the silicon sample. In designing the vacuum chamber to be used in our experiments, we have therefore provided an insulated feedthrough capable of supporting such a voltage.

Thus far, we have confined the discussion of the silicon surface to n-type material. The case of p-type Si is completely analogous. Figure 3 shows the possible band bending at the surface of p-material when the latter is covered by an inversion layer and immersed in a changing ambient.

There is one additional complication associated with electron irradiation of semiconductor surfaces. Besides being able to change ϕ_s and the nature of recombination sites on the surface, electrons can also induce a surface photovoltage which can change the energy relation between the quasi-fermi levels at the surface. The surface photovoltage can also be used to determine the absolute magnitude of the surface potential. Measurement of the absolute magnitude of the surface potential requires that the surface photovoltage be measured as a function of the intensity of the incident ionizing radiation. The value of the surface photovoltage tends toward saturation at a value equal to the diffusion potential difference between the bulk material and the surface.

REVIEW OF EARLIER EXPERIMENTS ON THE EFFECTS OF SUB-THRESHOLD ELECTRONS ON Ge AND Si

The results of a Brown University investigation of the effects of "sub-threshold" electrons on Ge and Si have been described in Refs. [9] and [10]. Those experiments can be summarized as follows.

Irradiation of Ge and Si by electrons whose energies are below the thresholds for bulk damage can lead to substantial changes in the short circuit current I_{sc} of photovoltaic cells exposed to strongly absorbed

light. These previous experiments were performed mainly in the vacuum produced by the oil diffusion pumps of the Van de Graaff accelerator which served as the source of electrons. In the case of n-Si, it was found that the irradiation caused increases in I_{sc} as shown in Fig. 4, while in the case of p-Si the changes were in the opposite direction as shown in Fig. 5. In these figures I_{sc} is plotted as a function of integrated flux in microcoulombs/cm² of 100 keV electrons. The curves shown in Figs. 4 and 5 exhibit a tendency to saturate. Interruption of irradiation led to a recovery of the surface from these irradiation effects. The rate of recovery was quite rapid; the surface achieved a stabilized state after about one-half hour of rest. Germanium surfaces behaved in essentially the same way: irradiation produced substantial changes which could be either increases or decreases in I_{sc} and the surface returned to a state resembling its earlier state when the irradiation was interrupted. The experiments with Ge exhibited yet another feature. In some cases, the rate of change was different during the early and later stages of irradiation. In some instances, even the direction of the change was different. The value of I_{sc} might first increase and after attaining saturation, it would decrease. This suggested that two processes may have been involved. The first of these would be a change in ϕ_s . This could then be followed by a change in the "fast" states, or in surface recombination velocity. Of course the experiments did not eliminate the possibility that the changes could be completely attributed to changes in ϕ_s . One purpose of the present research program is to distinguish between these possible reasons for changes in I_{sc} .

Another reason for this investigation is the question of the role played by the residual gases in the vacuum chamber. The Van de Graaff machine oil diffusion pumps provide a vacuum containing organic vapors which can form deposits on the semiconductor surfaces and can then be acted on by the electron beam. Irradiation of two silicon samples in an organic vapor free vacuum provided by sorption forepumps and an ion pump resulted in strikingly different behavior. The radiation induced surface changes proved to be more stable than they had been in the vacuum produced by the oil diffusion pumps; virtually no recovery was observed even after a ten hour rest. More experiments in organic vapor free vacua are needed to ascertain whether these results represent standard behavior of cells or whether they resulted from a special heat treatment to which the samples had been subjected.

Calculations based on even earlier experiments at Brown had shown that the changes in I_{sc} caused by these surface effects could lead to changes of as much as 10% in the output of silicon cells exposed to the violet-rich spectrum of outer space sunlight.

The fact that the changes can be in a desirable direction, i.e. that they can lead to an increase in I_{sc} , makes it desirable to try to establish the underlying cause of these changes. The fact that the experiments in the organic vapor free vacuum indicated that the surface had been stabilized as a result of irradiation provides another reason for acquisition of more information about the processes involved.

EXPERIMENTAL ARRANGEMENT

a. Design of an Irradiation Chamber

For the reasons cited above, it is necessary to perform experiments in an organic vapor free vacuum. In our earlier experiments, we used a glass-metal system in which we were able to achieve a vacuum in the range 10^{-7} - 10^{-8} torr by pumping with the Vac-Ion pump. That chamber suffered from the disadvantage that disassembly to change samples required unsoldering the parts of the system. This leads to some contamination.

In order to provide an improved irradiation chamber, an all metal vacuum irradiation chamber has been designed and constructed. An assembly drawing of the test chamber and sample dewar is shown in Fig. 6. Also, a photograph of the entire ultrahigh vacuum system is presented in Fig. 7 including the Varian Vac-Ion pumping station, and the bellows connecting the system to the Van der Graaff vacuum system.

The test chamber consists of an inverted stainless steel "tee" (see Fig. 6) with a Varian high vacuum flange at one end of the horizontal member and a specially designed electron beam "window" at the opposite end. The Varian flange is a standard commercially available item which seals via a copper gasket to a mating flange on the Vac-Ion pumping station. The electron beam window is a modified version of Ultek flange which is also copper gasket sealed, but has the feature that the flange surfaces which seat into the gasket are of the rounded edge type rather than the usual sharp edge edged flanges. We found by experiment that placing a thin nickel foil of 0.00015 inch thickness between one of the round flanges and the copper gasket allowed the flanges to be torqued together to the manufacturer's specifications without any damage to the foil. Such a system provides an easily replaceable beam "window" without the usual necessity of first brazing the foil to a ring of heavier material which can withstand the strains of the mounting system. This method of mounting also results in the foil being tightly stretched (like a drum head) which should contribute substantially to the uniformity of the beam after passing through the window.

The vertical leg of the tee is terminated with a commercially available flange, which mates to a similar flange on the sample carrying dewar discussed below. Although this flange system was originally designed for gold O-ring sealing, discussion with members of the staff of the Cambridge Electron Accelerator has resulted in the use of lead seals instead. Their experience has shown that Pb seals just as well and is considerably less expensive.

As shown in the drawing and photograph, a glass window is also provided on one side of the "tee"; this permits visual examination of the dewar cold finger when it is in place in the system. It also allows illumination of the specimen in the course of irradiation experiments. The window is also sealed via a Pb O-ring.

The sample dewar is of standard double wall construction with a liquid capacity of about 2 1/2 liters. This is sufficient to maintain

the cold finger near liquid nitrogen temperature for about 24 hours when the system is pumped down to the high vacuum range of 10^{-6} - 10^{-7} torr. The inner wall of the dewar terminator is a large (1 inch dia.) threaded stud onto which various sample mounting blocks can be screwed. While this will result in the loss of a few degrees in the ultimate low temperature obtainable on the samples, it was felt that, since a variety of experiments is anticipated in this system, the advantages of interchangeable mounting blocks outweighed this possible disadvantage. At present the mounting block consists of a right parallelepiped of square cross-section with two opposite faces provided with threaded mounting holes to secure samples to the block. The threaded mounting holes as well as the cold-finger-thread stud-hole have been vented to eliminate the possibility of virtual leaks in the system.

Electrical access to the sample is provided by two nine pin glass-to-metal seals and one high voltage connector. The high voltage terminal will make it possible to apply a transverse voltage of at least 500 V. The connectors are held in place by soft solder. The flange carrying the electrical penetrations is sealed to its mate with a lead O-ring.

Material and Assembly

The primary materials used throughout the construction are compatible non-magnetic stainless steels. Exceptions are as follows:

<u>Item</u>	<u>Material</u>
sample mounting block	oxygen free copper
Varian flange gasket	high purity copper
Ultek flange gasket	high purity copper
electron beam window	nickel foil
viewing windows	fused silica
dewar flange seal	lead O-ring
electrical penetration flange seal	lead O-ring
9-pin electrical feed-throughs	glass to tinned Kovar
MHV high voltage feed-through	glass to tinned Kovar
viewing window seat	lead O-ring

The assembly is fusion heli-arc welded using no fillit materials with the exception of the flange carrying the Ultek-window assembly which has a fillited butt joint.

After welding all the stainless steel parts of the system including the Vac-Ion pump components were cleaned and etched by the Diversy process giving extremely contamination free surfaces. All other components were also cleaned according to prescribed methods. The vacuum welds are individually inspected with a Veeco Helium Leak Detector and showed no detectable leak.

b) Experiments Aimed at "Sub-Threshold" Bulk Phenomena

Figure 8 is a photograph of the glass dewar used in the search for bulk effects associated with displacement of lithium atoms. The dewar vessel

terminates in a copper cold finger of 1 cm^2 cross-section which has four faces, each capable of accepting a $1 \times 2 \text{ cm}^2$ silicon photovoltaic cell.

The cells are soldered to metallized Al_2O_3 platelets which in turn were cemented to the copper cold finger with G.E. cement. This mounting procedure provided the cells with thermal contact to the cold finger and electrical isolation from it. It, therefore, becomes possible to measure the electron beam current absorbed in the silicon-solar cells and the value of I_{sc} .

The presence of defects is signalled by a change in the I_{sc}/I_B ratio. In our experiment, a two channel recorder was used to record I_{sc} and I_B simultaneously.

The experiment is to be performed at a temperature low enough to prevent diffusion of lithium ions. This was assured by keeping the sample at liquid nitrogen temperature throughout the irradiation.

c) Modifications to the Van de Graaff System

The Van de Graaff beam will be scattered over an area somewhat larger than the sample with the help of an electrostatic deflection system and circuits designed to provide varying high voltage signals to the horizontal and vertical deflection plates at two incommensurable frequencies. The circuits required some redesign since the older version circuits were not operating as required.

CONCLUSIONS

1. The effect of irradiating semiconductors by electrons whose energy is too low to displace host lattice atoms were reviewed. In the case of lithium-doped silicon cells, such sub-threshold electrons could displace lithium ions and atoms, and thereby produce bulk defects into the silicon. The low atomic mass of the lithium atom (At. Wt. = 6) relative to that of silicon (At. Wt. \approx 28) suggests that lithium atoms could be displaced by electrons of 30 keV or even lower energy.

2. The effects of electron radiation on the semiconductor surface were reviewed. Electron irradiation can change both the surface potential ϕ_s , and the nature and concentration of recombination sites on the semiconductor surface. Experiments designed to separate these effects were described.

3. A steel chamber to allow irradiation of samples in an organic vapor free vacuum pumped by ion pump has been designed and constructed.

4. An experimental apparatus for studying effects of radiation in lithium-doped cells was described.

REFERENCES

1. H. Flicker, J. J. Loferski and J. Scott-Monck, Phys. Rev., 128, 2557-63 (1962).
2. R. L. Novak, Thesis, University of Pennsylvania (1961).
3. See for example: F. Seitz and Koehler in "Solid State Physics" (Edited by F. Seitz and D. Turnbull), Academic Press, New York, New York, 2 (1952).
4. R. A. Berger, H. Horiye, J. A. Naber, B. C. Passenheim, Quart. Rept., Gulf General Atomic Inc., JPL Contract 952387, p. 7 (October 10, 1969).
5. J. A. Naber and H. James, Bull. Am., Phys. Soc., 6 (1961).
6. E. O. Johnson, Jour. Appl. Phys., 28, 1349-53 (1957).
7. E. O. Johnson, RCA Review, 18, 556-570 (1957).
8. D. T. Stevenson and R. J. Keyes, Physica, 20, 1041 (1954).
9. J. J. Loferski, W. Giriat, I. Kasai and H. Flicker, Proc. Toulouse (France) Symposium on Effects of Radiation of Semiconductor Devices (June 1967).
10. See for example: I. Kasai, M.S. Thesis, Brown University, August 1966. The work was reported under NASA Grant NGR-40-002-026.
11. A. Marry and D. Gerlick, Phys. Rev., 107, 404 (1957).
12. G. C. Dousmanis, Jour. Appl. Phys., 30, 180 (1959).

jmm
gb
11/24/69

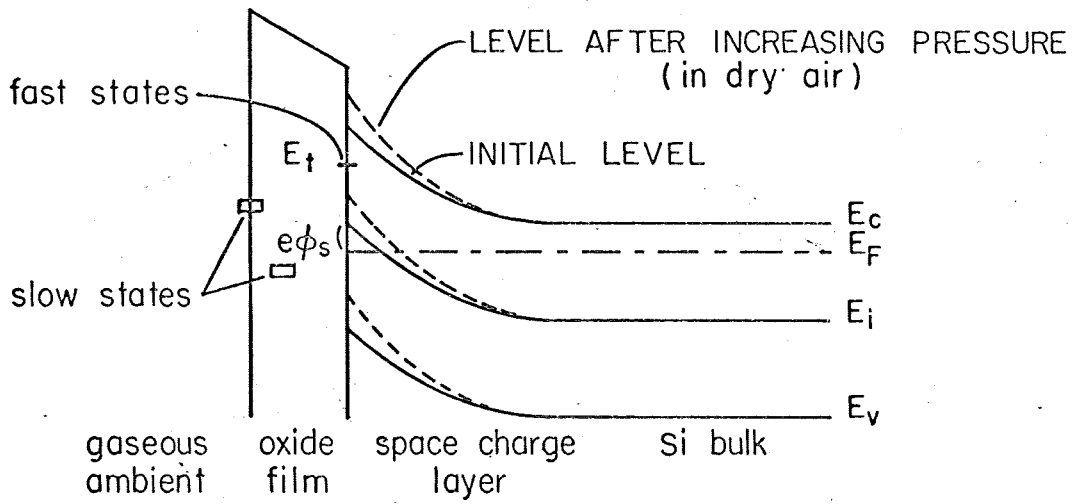


FIG. 1 ENERGY LEVEL DIAGRAM FOR n-Si SURFACE

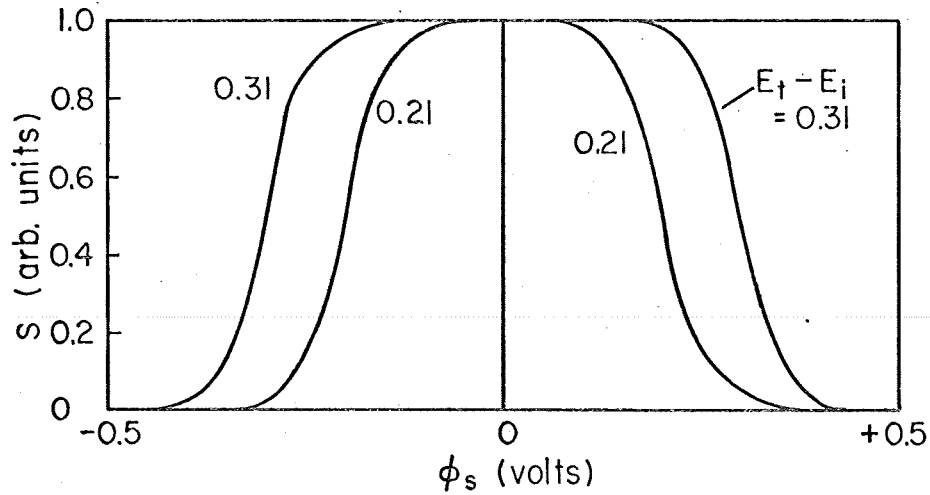


FIG. 2 RELATIVE VALUES OF S VS. ϕ_s

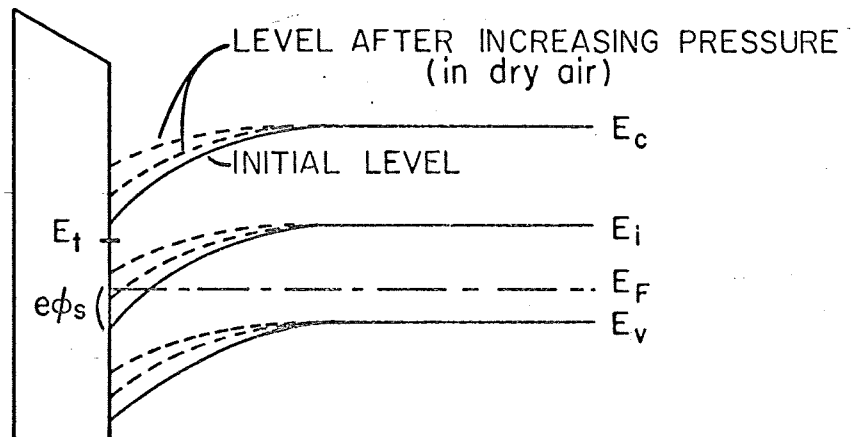


FIG. 3 ENERGY LEVEL DIAGRAM FOR p-Si SURFACE

n-TYPE Si; $\rho = 1\Omega - \text{cm}$

115 KeV; ① $I_B = 8\mu\text{A}/\text{cm}^2$

② $I_B = 8\mu\text{A}/\text{cm}^2$

③ $I_B = 8\mu\text{A}/\text{cm}^2$

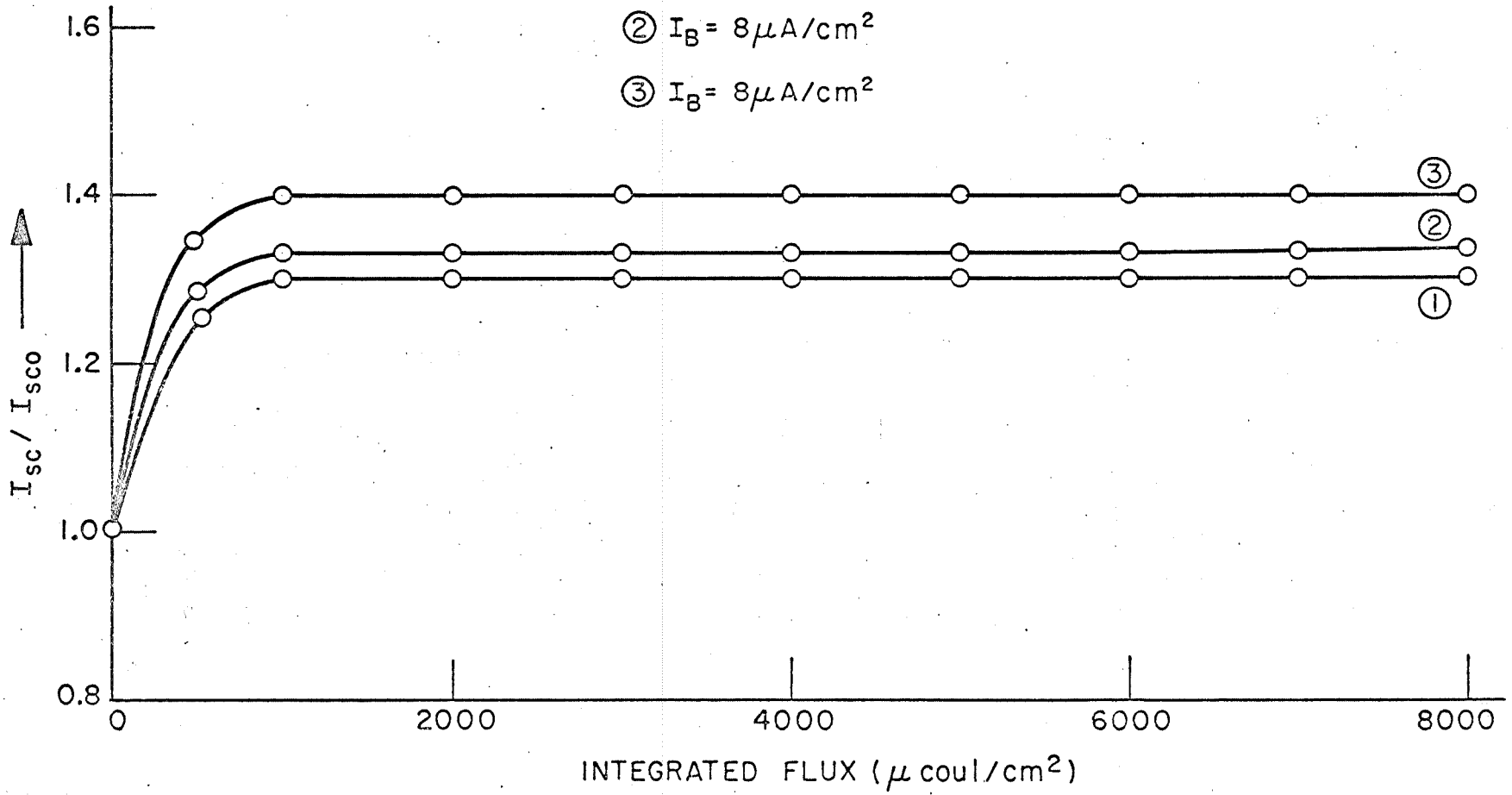


FIG. 4

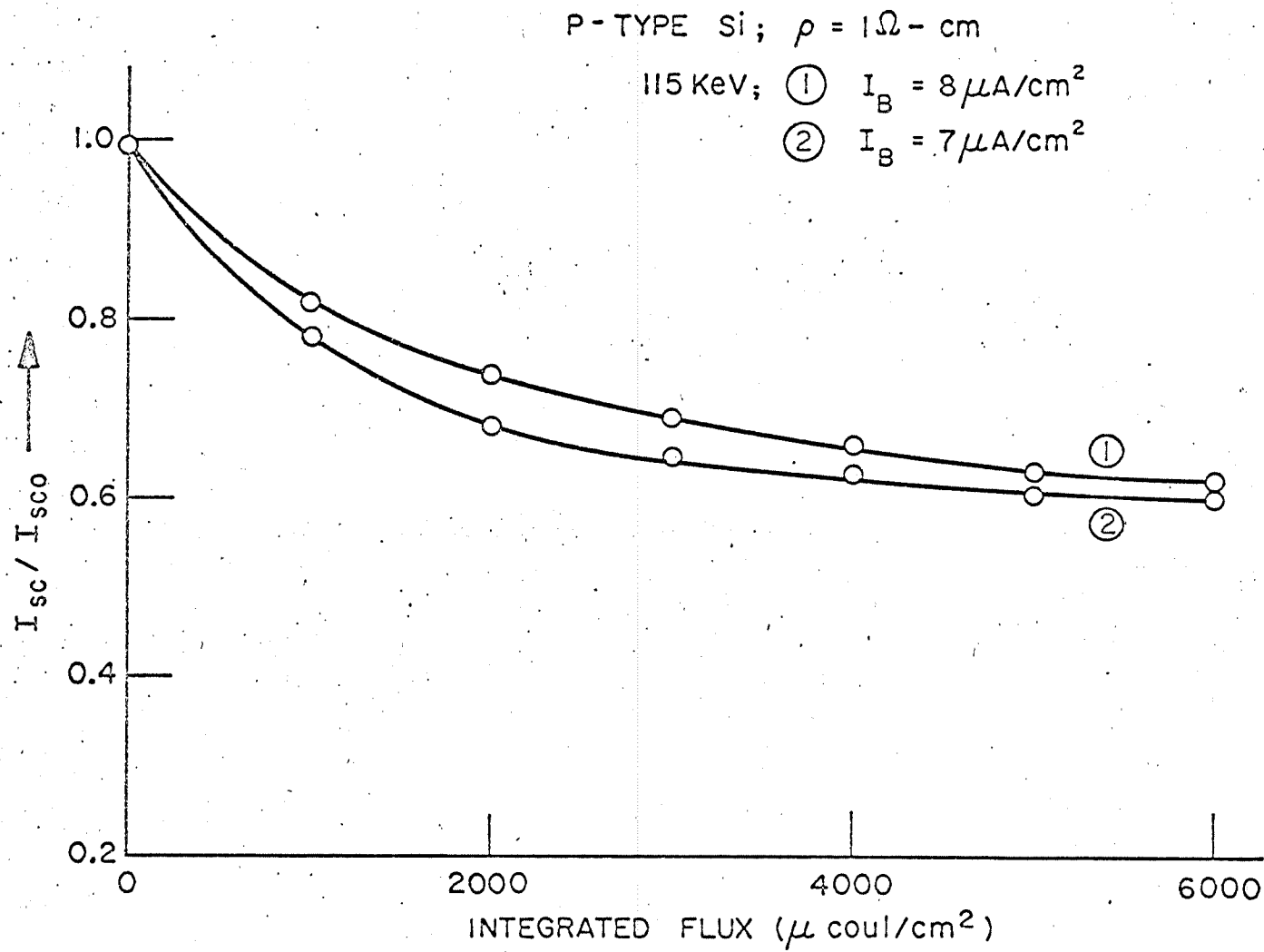
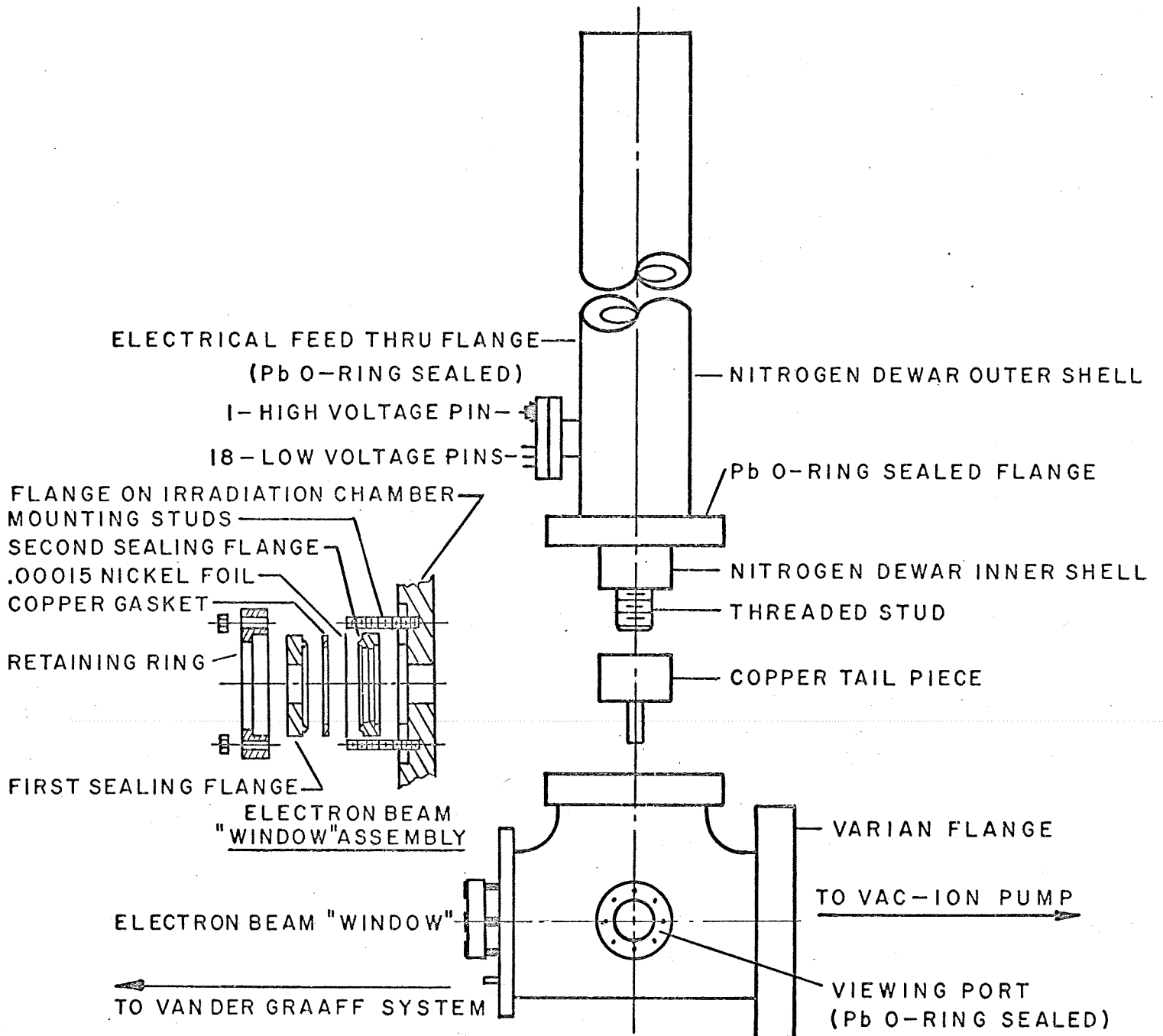


FIG. 5



APPROX. SCALE 1/4" = 1"

FIGURE 6

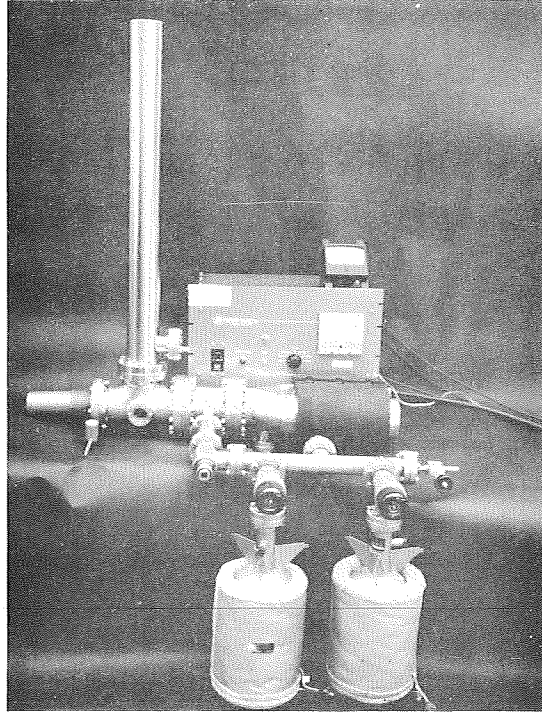


FIGURE 7

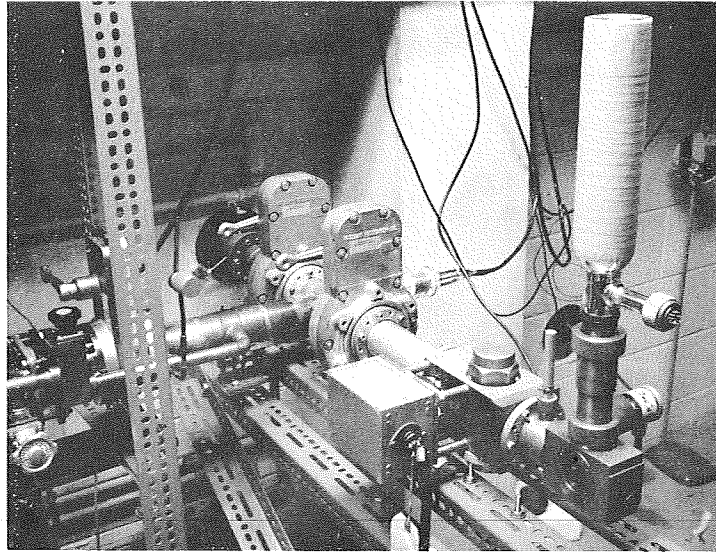


FIGURE 8